

Moisture sorption and diffusion in historical cellulose-based materials

Arkadiusz Kupczak  · Łukasz Bratasz · Joanna Kryściak-Czerwenka · Roman Kozłowski

Received: 22 December 2017 / Accepted: 2 April 2018 / Published online: 5 April 2018
© The Author(s) 2018

Abstract Moisture adsorption and diffusion were examined in 17 samples of historical and modern papers and cardboards, differing in the time of production and the pulping process. The moisture adsorption data for paper materials made of rags, gelatin-sized were close to each other whereas wood-pulp papers showed higher intra-group variability due to varying contents of lignin and rosin sizing. The average adsorption curve for all specimens was close to that of pure cellulose. In-plane diffusivities along the paper sheets in a stack, primary direction of uptake and release moisture by library objects, were determined as a function of relative humidity and paper

compression. Typically, the in-plane diffusivities fell within the range of 6×10^{-6} – 1.7×10^{-5} m²/s and were significantly affected by the paper fraction in the specimens which were combination of paper sheets and thin air layers or pockets between the sheets. The external mass transfer coefficient at the surface of the paper objects perpendicular to the paper sheets exceeded 2×10^{-3} m/s and significantly depended on the intensity of air motion in typical environments. Effective use of the adsorption and diffusion information obtained was demonstrated in modelling buffering capacities of books.

Keywords Moisture · Sorption · Diffusion · Cellulose · Historical paper · Libraries

Electronic supplementary material The online version of this article (<https://doi.org/10.1007/s10570-018-1772-9>) contains supplementary material, which is available to authorized users.

A. Kupczak (✉) · J. Kryściak-Czerwenka · R. Kozłowski
Jerzy Haber Institute of Catalysis and Surface Chemistry,
Polish Academy of Sciences, Niezapominajek 8, 30-239,
Kraków, Poland
e-mail: nckupcza@cyf-kr.edu.pl

Ł. Bratasz
The National Museum in Krakow, al. 3 Maja 1, 30-062,
Kraków, Poland

Present Address:

Ł. Bratasz
Institute for the Preservation of Cultural Heritage, Yale
University, PO Box 27395, West Haven, CT 06516, USA

Introduction

In the recent years, much attention has focused on managing indoor environments in museums, libraries and archives in a responsible manner, especially in terms of reducing energy use and carbon emissions (Hong et al. 2012; Staniforth 2014). The interest in the issue has been driven by the idea of ‘greening’ memory institutions so that they maintain high standards of collection care, while respecting the natural environment and resources. Cellulose-based materials such as paper and cardboard contained in books, manuscripts, historical records, prints and drawings

are vulnerable to temperature and relative humidity (RH) and therefore scientific understanding of how storage conditions ultimately affect these materials is crucial to the development of rational guidelines for the long-term control of climate in the repositories.

Research into climate-related issues of the preservation of paper materials has so far predominantly focused on hydrolysis and oxidation of cellulose (Strlič 2015), as well as risk of microbiological activity starting above 60% RH (Sedlbauer 2002). However, there are two further important consequences of paper's capacity to gain moisture when the RH is high, or losing moisture when the surrounding air is dry. On one hand paper collections act as moisture buffers reducing RH fluctuations in the repositories, on the other paper objects experience dimensional response—they shrink as they lose moisture and swell when they gain moisture. Paper objects may experience uneven moisture distribution, and consequently uneven dimensional change, in response to the RH variations as the moisture diffusion into or out of the object is not instantaneous. The stress induced by the uneven response will manifest by deformation like curls and cockles. Obviously, paper may also experience stress because of restraint on its dimensional response resulting from binding it into a book block or mounting into a rigid protective system.

The two key parameters—water sorption isotherms relating RH and the equilibrium moisture content (EMC) for a material, and coefficients of water vapour diffusion and mass transfer on the paper surface—need to be examined to understand the material buffering and moisture response.

In the range between 0 and 85% RH, which is of interest for the preservation of paper collections indoors, the relationships between EMC in paper and RH is described by a sigmoid shape of the type II isotherm in the IUPAC 1985 classification (Sing et al. 1985). It indicates the monolayer-multilayer physisorption in which an adsorbed surface layer progressively thickens as the vapour pressure is increased up to saturation pressure. At high RH values, the monolayer-multilayer adsorption path can be accompanied by a more rapid increase in sorbed water due to the processes of capillary condensation in the porous structure. The Guggenheim-Andersen-de Boer (GAB) three-parameter sorption equation has been used to interpret the physisorption of water on paper as it is capable of describing the full shape of

type II isotherm and yields meaningful physical parameters as monolayer capacity and energy constant related to the net molar heat of adsorption (Timmermann 2003; Parker et al. 2006; Bedane et al. 2015).

Moisture diffusion in paper occurs through three principal pathways: diffusion of water vapour in the pore space, diffusion of water in the condensed form within cellulose fibres and the moisture exchange (adsorption or desorption) between the fibres and the pore space (Ramarao et al. 2003). Whilst vapour transport through the pore space dominates at low RH levels, diffusion of the condensed phase can be significant at high humidity conditions. The effective diffusivity of moisture in the paper, the outcome of the three diffusion mechanisms, can be determined experimentally by measuring the total flux of moisture driven by water concentration gradient through a stack of paper under steady-state conditions (Gupta and Chatterjee 2003a). The effective moisture diffusivity established from the steady-state moisture flux measurements was found to predict also moisture transport in paper stacks subjected to ramp changes of the external RH, especially for low speeds of the changes, characteristic of RH variations in museum or library repositories (Gupta and Chatterjee 2003b). This indicates that, under slow RH variations, the exchange of moisture between the pore space and fibres is faster than moisture diffusion that is to say equilibrium moisture content is constantly attained in the fibre phase.

In this study, moisture sorption isotherms and water vapour diffusion and mass transfer coefficients were determined for a selection of specimens of historical papers and cardboards, dated to between the seventeenth and twentieth centuries. The composition of paper-based materials housed in the library and archival repositories reflects the paper production processes changing during the centuries. Since its beginning in the medieval times until well into the nineteenth century, the European paper making used linen, hemp and cotton rags as the source of the cellulosic material. To render the formed paper sheets water repellent and thus suitable for writing, they were sized with gelatine extracted from various animal tissues containing collagen. Only in the second half of the nineteenth century, wood fibres become dominant in the paper production, generally, either as mechanical or chemical pulp. Mechanical pulping methods involved mechanical separating the cellulose fibres

from one another leaving much of the lignin in the material. The mechanical pulp was used for low-cost products as newsprint or paperboards. In turn, chemical pulping involved chemical degradation of lignin and hemicellulose which could be removed from the cellulose. Alum-rosin size invented in 1807 gradually replaced the gelatin size due to its lower cost.

To reflect varying paper characteristics which may be encountered in typical archival and library repositories, three principal types of historical paper-based materials indicated above were investigated in this study: gelatin sized papers made of rags and rosin-alum sized wood pulp-based papers obtained in the mechanical or chemical pulping process. The study focused on establishing experimentally parameters useful in modelling the ‘real-time’ moisture movement in the historical paper objects in response to RH variations. The parameters comprised average GAB constants obtained by fitting water vapour sorption data for several paper types, characteristic of mixed paper collections, and effective diffusivities both in transverse and planar directions that is to say across the paper stack and along the paper sheets in a stack, as books or records placed next to each other on a bookshelf significantly absorb/desorb water vapour from the surrounding space only along this direction.

Materials and methods

17 samples of historical and modern papers and cardboards, differing in the time of production and the pulping process, were used in the testing programme. Details of the materials along with their photographs are given in Online Resource 1.

FT-IR spectra were recorded using a Nicolet 6700 FT-IR spectrometer, equipped with the Smart Ark Accessory (ZnSe crystal). Spectral analyses were performed at a resolution of 4 cm^{-1} in the range of $4000\text{--}650\text{ cm}^{-1}$, collecting 64 scans at the room temperature and ambient humidity.

Moisture adsorption and desorption isotherms were determined at $24\text{ }^{\circ}\text{C}$ and for a range of RH between 0 and 80%. The measurements were done gravimetrically with the use of a vacuum microbalance from CI Electronics, UK. Typically, a 0.1 g piece of a material was weighed and outgassed prior to a measurement under a vacuum of a residual pressure less than 0.1 Pa. The aim was to eliminate water physisorbed during the

storage of the sample. A vacuum was maintained until a constant weight was obtained, then subsequent portions of water vapour were introduced, and the respective mass increases due to the sorption and the respective equilibrium pressures were recorded. Samples were considered to have reached an equilibrium when the weight changes were less than 0.05% in 40 min. The equilibrium moisture contents were calculated on the basis of the initial weight of the out-gassed sample.

The experimental set-up proposed by Mosequette et al. (2005) was used for measuring the external mass transfer coefficient and the water vapour diffusivity of paper materials in the through-plane (transverse) direction—shortly D_z . Round Plexiglas diffusion cups were provided with a step machined into the wall so that circularly-cut paper sheets of 60 mm in diameter could be placed in them and held by the Plexiglass ring, screwed into the cup. The connection was sealed by wrapping polytetrafluoroethylene (PTFE) tape around the ring’s thread and spreading a silicone sealant over the rim of the cup and the ring. In accordance with the ASTM E96/E96-M standard (2016), the cups were partially filled with distilled water (the water method) or anhydrous calcium chloride (the desiccant method) to obtain nearly dry or fully saturated with water vapour, respectively, air inside. The cups were placed inside a climatic chamber controlling the temperature at $22\text{ }^{\circ}\text{C}$ and RH at 50% so that the required difference in water vapour pressure across the paper specimens was obtained. An additional measurement was done using the desiccant method but at RH of 70% in the climatic chamber.

Stacks of paper sheets varying from 30 to 90 were investigated, to obtain relationships between water vapour permeability and stack thickness—the diffusion path length. In a single experiment involving a specific RH difference, the weight changes of two or three cups comprising specimens of a given thickness were measured. The weighing was started 48 h after placing cups inside the climate chamber, to ensure that paper specimens had reached a state of dynamic equilibrium, and was repeated in one or two day intervals until a satisfactory number of experimental values were obtained.

A different diffusion cup was used for measuring the diffusivity in the in-plane direction—shortly D_{xy} (Mosequette et al. 2005). A set of paper circles of

radius of 30 mm were cut with concentric holes of diameter of 10 mm equal to the inner diameter of the diffusion cup. The sheets were sandwiched together by a plate placed on the top of the stack. In an additional experiment, the stack thicknesses was reduced by compressing the same number of paper sheets with clips to imitate more adequately the fact that in reality books stored on a bookshelf may be squeezed with a varying degree of tightness.

An uptake of water vapour by two book specimens in response to an RH step change from dry condition to approximately 43% was measured gravimetrically in a plastic container or in a climatic chamber in which constant RH and temperature of 22 °C was maintained. One book specimen was made of Eighteenth century gelatin-sized rag-based paper—190 mm (length) × 195 mm (width) × 11.5 mm (thickness) and the other of Nineteenth century machine-made paper—203 mm (length) × 125 mm (width) × 23.4 mm (thickness). The covers and spine of the specimens was made impermeable to water vapour so that only three remaining side surfaces were left open to the water vapour transport. Prior to the experiment, each book specimen was dried at 105 °C to assure the removal of water physisorbed.

The numerical modelling of moisture transport in the book specimens was carried out using COMSOL Multiphysics. The software allowed the time dependent water vapour diffusion equation to be solved using finite element modelling.

Results and discussion

Composition of paper materials investigated

Historical papers and boards manufactured prior to 1800 were confirmed to be gelatin sized materials made of rags. Following the practice of protein analysis using FTIR, gelatin was identified in all these materials by the amide I and II bands, near 1650 and 1550 cm^{-1} , associated with C=O stretching vibration and C–N stretching and N–H bending vibrations of peptide groups (Rouchon et al. 2010) (Fig. 1).

In turn, rosin sizing was identified in the nineteenth and twentieth century papers by a double signal in the range of 1606–1612 cm^{-1} characteristic of C=C stretching in conjugated structures included in the ring systems of rosin as well as the near 1710 cm^{-1}

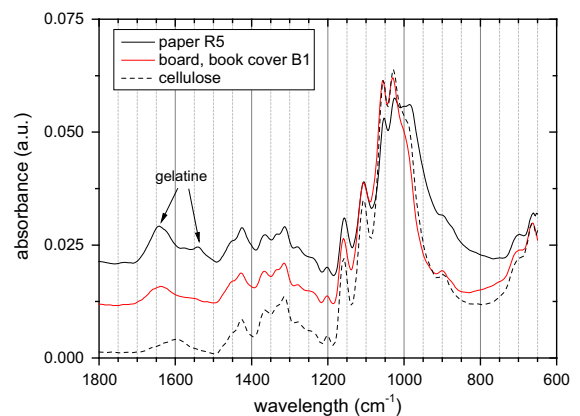


Fig. 1 FTIR spectra of historical paper (R5) and board (B1) made of rags and gelatin sized. The spectrum of pure microcrystalline cellulose is shown for comparison

signal due to the COOH vibration of abietic acid (Calvini and Gorassini 2002) (paper M1 in Fig. 2). Further, the wood pulp paper materials containing lignin could be identified by bands at 1510, 1580 and 1605 cm^{-1} characteristic of aromatic structures present in lignin (board B2 in Fig. 2). The spectra of rosin and lignin overlap in the 1550–1650 cm^{-1} range but bands at 1510 cm^{-1} (lignin) and 1710 cm^{-1} (rosin) remain clear markers of the components in rosin-sized lignin-containing papers (paper W1 in Fig. 2). The infrared spectra of all paper-based materials investigated are contained in Online Resource 2 and the types of the materials used in the study are summarized below in Table 1.

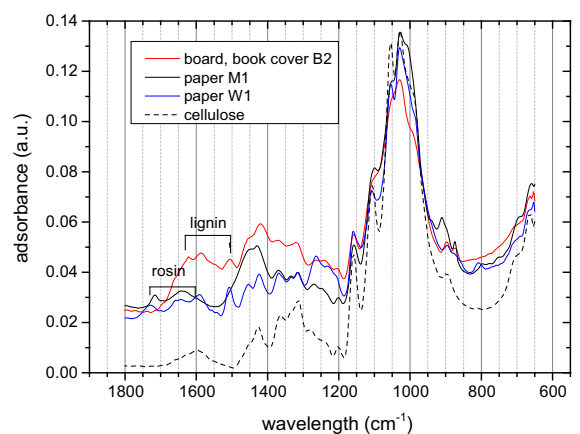


Fig. 2 FTIR spectra of lignin-free (M1) and lignin-containing (W1) wood pulp papers, rosin/alum sized, as well as unsized lignin-containing board (B2). The spectrum of pure microcrystalline cellulose is shown for comparison

Table 1 Average GAB constants obtained from the regression of the sets of adsorption data available for groups of the specimens

Material type	Number and codes of the specimens	'Average' GAB parameters for groups of specimens			
		V_m (%)	c	k	R-squared
Paper materials made of rags, gelatine sized	6 (R1–R5, B1)	4.39	13.3	0.72	0.96
Machine-made paper materials	9 (M1–M4, W1–W4, B2)	4.66	13.1	0.64	0.82

Adsorption isotherms of water vapour

The relationship between the amount of water adsorbed on the paper materials and RH is described by the three-parameter Guggenheim-Andersen-de Boer (GAB) equation:

$$EMC(RH, T = const.) = \frac{V_m \times c \times k \times RH/100}{(1 - k \times RH/100) \times (1 + (c - 1) \times k \times RH/100)} \quad (1)$$

where EMC is the equilibrium moisture content in percent, RH—relative humidity in percent, V_m —the monolayer capacity in the same units as EMC, c —an energy constant related to the difference of free enthalpy (standard chemical potential) of water molecules in the upper sorption layers and in the monolayer, and k —the third parameter, related in turn to the difference of free enthalpy of water molecules in the pure liquid and the upper sorption layers.

The specific surface area s_{GAB} is obtained from the monolayer capacity V_m :

$$s_{GAB} = V_m \times \rho \times L \times \sigma / M \quad (2)$$

where M is the molar mass of water, ρ is water density, L is the Avogadro number and σ is the average area occupied by one water molecule in the monolayer— 0.114 nm^2 was used in this study.

By way of example, the experimental data for water vapour sorption by a gelatin-sized rag paper are compared in Fig. 3 with curves calculated using the GAB equation. For the desorption branch, the hysteresis effect is observed i.e. higher moisture content during desorption when compared to that during adsorption at any given RH value. This phenomenon is associated with the swelling of a non-rigid cellulose structure in the course of adsorption, so that the effect is in fact a manifestation of elastic hysteresis (Sing

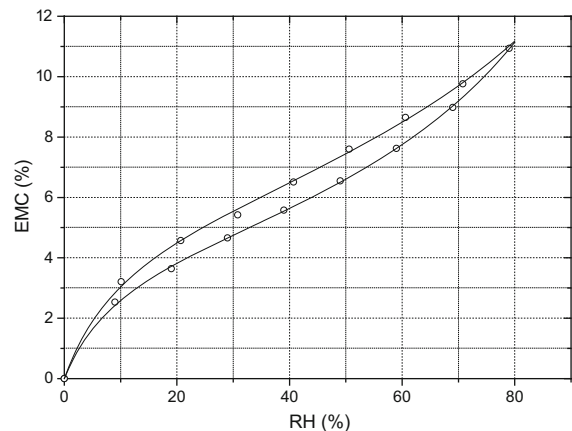


Fig. 3 The experimental data for water vapour adsorption and desorption by gelatin-sized paper made of rags (R3) are compared with the curves calculated from the least-square regression of the data to the GAB equation

et al. 1985). The GAB constants were determined by a least-squares regression of the GAB relation for $0\% < RH < 80\%$, which fully covers RH conditions relevant for the preservation of paper-based materials indoors. The regression was performed separately for the adsorption and desorption branches. It should be noted that the adsorption branch only yields meaningful monolayer capacity, and consequently specific surface area, owing to the hysteresis loop between the adsorption and desorption branches. The GAB constants and s_{GAB} values determined for all paper materials investigated are contained in Online Resource 1.

Further to the analysis of sorption data for the individual paper materials, average GAB constants were obtained by fitting, to the GAB equation, the entire sets of adsorption and desorption data available for two broad groups of the materials analysed. The first group comprised gelatin sized materials made of rags (Fig. 4) and the other wood pulp-based papers obtained in the mechanical or chemical pulping

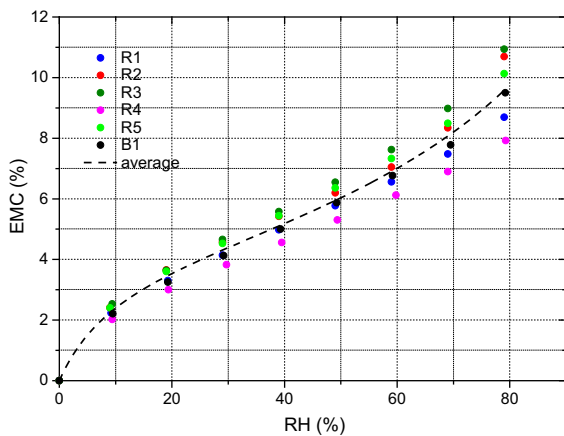


Fig. 4 The experimental data for water vapour adsorption by gelatin-sized paper materials made of rags—modern laid paper (R1), four historical papers (R2–R5) and paperboard in a book binding (B1)—are compared with the average curve calculated from the least-square regression of the data to the GAB equation

process, therefore varying in the lignin content, alum/rosin sized, though one specimen (B2) was unsized (Fig. 5). The respective GAB constants for the average relationships and R-square values for the two groups are given in Table 1.

Calculating the best fit average RH-EMC relationships for a number of specimens belonging to a specific groups of objects allowed the intra-group variability—reflected in the R-squared value—to be analysed. The moisture adsorption data for paper

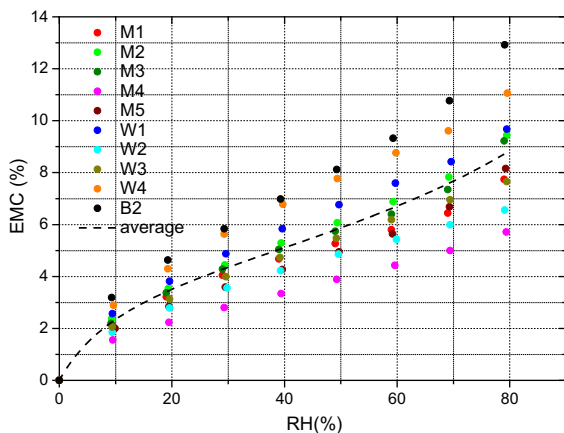


Fig. 5 The experimental data for water vapour adsorption by machine-made paper materials—alum/rosin sized papers of varying lignin content (M1–M5 and W1–W4) and lignin-containing unsized paperboard in a book binding (B2)—are compared with the average curve calculated from the least-square regression of the data to the GAB equation

materials made of rags, gelatin-sized are close to each other as indicated by high R-squared value of 0.96. Conspicuously, the average adsorption curve for this category of paper materials is very close to that of microcrystalline cellulose (Fig. 6) which is a pure cellulose powder adopted as a certified reference material in the procedure for the determination of water sorption isotherms, especially of foods (Jowitt and Wagstaffe 1989). Also adsorption curves of contemporary ‘museum’ boards, used in museum, archive or library storages for mounting paper objects, box making or book binding, are close to the average curve analysed, as the materials consists of cotton fibres built of almost pure cellulose (Fig. 6). Gelatin used as the size does not alter the water sorption characteristics of the paper as it is a hygroscopic material and the amount adsorbed in the RH range of 0–80% is similar that of the cellulose (Rachwal et al. 2012). Therefore, generally, the moisture sorption curves of the papers are dominated by the sorption of the cellulose only slightly modified by impurities or the glue.

In contrast, the water adsorption characteristics of wood-pulp papers showed higher intra-group variability reflected in a lower R-squared value of approximately 0.8. The reason for the increased variability lies in the opposing effects of alum/rosin sizing on one hand and presence of lignin in the paper on the other, on the water vapour adsorption properties of the

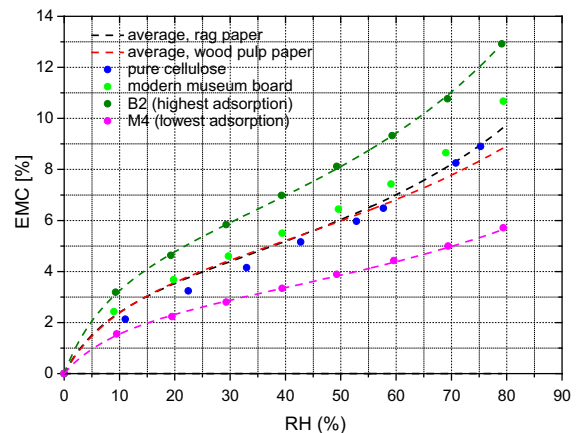


Fig. 6 The experimental data for water vapour adsorption by microcrystalline cellulose and contemporary museum board (B3) are compared with the average adsorption curves for rag and wood pulp paper materials. Adsorption curves of the highest (B2) and lowest (M4) adsorption are provided to define the upper and lower limits of adsorption by paper collections

papers. Rosin-sizing imparts water-repellent properties to the paper and, hence, reduces hydrophilic surface of cellulose available for the water adsorption (Hubbe 2011). Lignin in turn shows higher water adsorption than cellulose in the entire RH range (Rawat and Khali 1999; Volkova et al. 2012). As the result, machine made paper materials used in the same book printed in 1898 exhibited the highest and the lowest water vapour adsorption by lignin-rich unsized paperboard in the binding and lignin-free, alum/rosin sized paper, respectively, measured in this study (Fig. 6). Notwithstanding the increased variability among the machine-made paper materials, the average adsorption curve for this group of specimens is again very close to that of the rag papers and pure cellulose. Such generalized adsorption information can be useful in modelling buffering capacities of library and archival collections by quantifying ‘real-time’ moisture movement across the paper objects of varying shape and thickness with the use of the finite element method—the modeling being based on experimentally determined material properties: adsorption/desorption of water vapour, water vapour diffusion and external mass transfer coefficients. Further, constantly varying uptake and release of moisture from paper collections can be coupled to the modelling of indoor microclimate and energy consumption in collection storage spaces with the use of the building simulation software (Kupczak et al. 2018).

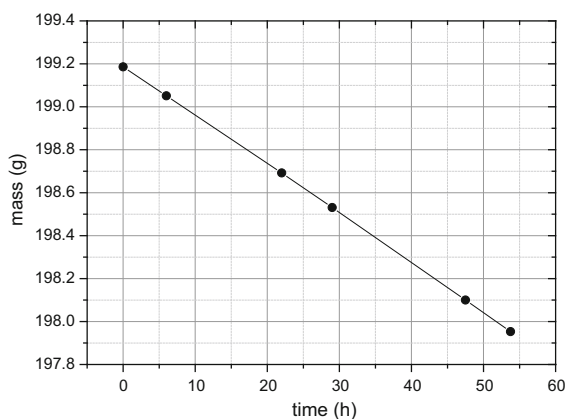


Fig. 7 Mass loss of water in a diffusion cup due to water vapour flow through 6.6 mm layer of paper M4, temperature and RH in the climatic chamber were 22 °C and 50%, respectively

External mass transfer coefficient

Figure 7 shows an exemplary plot of mass loss of water contained in a diffusion cup, due to a steady state water vapour flux through the paper stack driven by the RH gradient of 50% (the water method). The water vapor transfer rate (WVTR, kg/s) through the specimen was determined as a slope of the linear relationship between specimen’s mass and elapsed time.

Knowing the WVTR, one can calculate the material water vapour transfer resistance Y (in s/m):

$$Y = A\Delta c/\text{WVTR} \quad (3)$$

where A is the surface through which the water vapour is transported ($2.8 \times 10^{-3} \text{ m}^2$), and Δc is the gradient of water vapour concentration in air (in kg/m^3) driving the water vapour flux— Δc can be calculated from the RH gradient assuming the ideal-gas law:

$$c = \left(\frac{\text{RH}}{100}\right) p_{\text{sat}}(T)M_{\text{water}}/(RT) \quad (4)$$

where $p_{\text{sat}}(T)$ is the saturated water vapor pressure at a given temperature (2642 Pa at 295 K), R is the gas constant ($8.3145 \text{ Pa m}^3/\text{mol K}$), T is temperature (295 K) and M is molecular mass of water (0.018 kg). Plotting a water vapor transfer resistance against the specimen thickness H (in m) allowed two key parameters describing the moisture transport through the material to be found (Fig. 8):

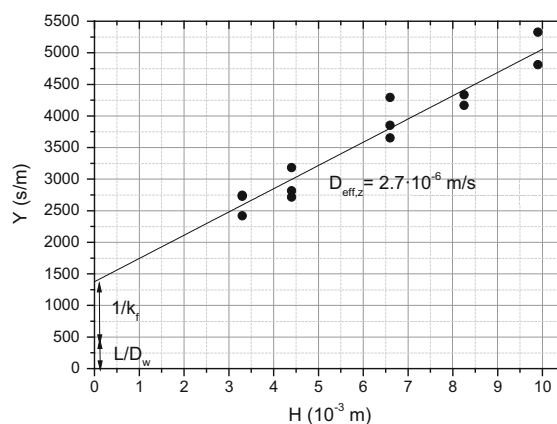


Fig. 8 Overall water vapour transfer resistance Y in the diffusion measurements versus the paper (M4) stack thickness H

$$Y = H/D_z + R_0 \quad (5)$$

the effective material diffusivity D_z (in m^2/s) as an inverse of the slope and R_0 —sum of water vapour transfer resistance above and below of the specimen top and bottom surfaces, acting in series, as the intercept (zero specimen thickness):

$$R_0 = L/D_w + 1/k_f \quad (6)$$

where L is the thickness of the air layer in the diffusion cup between the surfaces of water or desiccant and the bottom face of the paper sample—kept at approximately 13 mm, D_w is the water vapour diffusivity in quiescent air at the experimental temperature ($2.7 \times 10^{-5} \text{ m}^2/\text{s}$ at $T = 295 \text{ K}$), and k_f is the external mass transfer coefficient (on the outside paper surface). It should be noted that the effect of convective currents in the diffusion cups was neglected.

Figure 8 shows a plot of the water vapour transfer resistance Y versus the paper stack thickness for the RH gradients of 50% produced by water or the desiccant, respectively. Since the plot is linear, the external resistance R_0 could be determined by extrapolating a linear least-square fit to the data to the intercept (zero specimen thickness). If the resistance of the air layer in the diffusion cup between the bottom surface of the sample and the surface of water or desiccant L/D_w (480 s/m) is subtracted, the resistance of the external boundary layer or $1/k_f$ is obtained ($k_f = 1.1 \times 10^{-3} \text{ m/s}$ for the analysed case).

The mass transfer resistance in the boundary layer adjacent to the top surface of the paper samples is affected by the air movement surrounding the diffusion cups. To quantify this influence, two further measurements of D_z and k_f were carried out. In one experiment, the diffusion cups containing water were placed in a large glass desiccator with saturated water solution of potassium carbonate with an equilibrium RH of 43%. It was assumed that this configuration

produced nearly quiescent air adjacent to the surfaces of the test specimens, which would mimic environments with little air circulation. In the other experiment, the diffusion cups were placed in the climatic chamber close to a fan forcing air circulation which would imitate environments with considerable air motion. The D_z and k_f values obtained in the experiments are listed in Table 2 with 95% prediction intervals about the k_f value.

As expected the mass transfer coefficient was the greatest when the specimens were placed closed to the operating forced air-circulation system in the chamber, and the smallest for the measurement in the desiccator. The tendency and the ranges agree well with external mass transfer coefficients for paper specimens determined previously using various experimental approaches. For the diffusion cups placed in climatic chambers, minimal values of the coefficient were estimated at $1.2\text{--}1.8 \times 10^{-3} \text{ m/s}$ from the analysis of profiles of RH or moisture content in the paper samples under the steady-state water vapour transport (Gupta and Chatterjee 2003a; Massoquete et al. 2005). In a later paper, Chatterjee (2008) reported higher values of the coefficients ($2\text{--}2.8 \times 10^{-3} \text{ m/s}$) from similar measurements but under unsteady-state transport of moisture. A similar value of $2.5 \times 10^{-3} \text{ m/s}$ was determined from measurements of liquid water evaporation in a chamber (Bandyopadhyay et al. 2000). In turn, Bedane et al. (2016) derived an average value of $3 \times 10^{-3} \text{ m/s}$ from measurements of transient moisture uptake rates by paper materials over a wide range of RH. $7 \times 10^{-3} \text{ m/s}$ (Bandyopadhyay et al. 2002; Nilsson et al. 1993) were maximum values of the coefficient reported.

The effective paper diffusivity of approximately $2 \times 10^{-6} \text{ m}^2/\text{s}$ agrees well with values determined for relatively porous papers of low density between 500

Table 2 Water vapour diffusivity of paper M4 in the through-plane direction D_z and external mass transfer coefficient k_f

Environment of the diffusion cups	Airflow rate (m/s)	D_z ($10^{-6} \text{ m}^2/\text{s}$)	k_f with 95% prediction interval (10^{-3} m/s)
In the middle of a climatic chamber	0.15	2.7	1.1 (0.5–5)
In a climatic chamber close to a fan forcing air circulation	0.35	2.0	1.6 (> 0.7)
In a glass desiccator	Stagnant air	2.1	0.7 (0.4–1.6)

and 800 kg/m³ (Massoquete et al. 2005; Nilsson and Stenström 1995).

Effective diffusivity in the in-plane direction

The in-plane diffusion through the cylindrical paper stack used in the experiment occurs along the radial dimension and the effective diffusivity is calculated using the following equation derived from the steady-state diffusion equation in cylindrical coordinates (Massoquete et al. 2005):

$$D_{xy} = \ln\left(\frac{r_{outer}}{r_{inner}}\right) / \left(2\pi H \left(\frac{\Delta C M_{water}}{WVTR} - R_0\right)\right) \quad (7)$$

where r are the outer and inner radii of the paper cylinder, 30 and 10 mm, respectively, and:

$$R_0 = \frac{L}{D_w \pi r_{inner}^2} - \frac{1}{k_f 2\pi r_{outer} H} \quad (8)$$

Derluyt et al. (2007) estimated the values of external mass transfer coefficient k_f for surfaces of paper stacks perpendicular to the paper sheets by measuring transient moisture uptake rates in the in-plane direction for two specimens imitating books differing in paper fractions (0.9 and 0.6) in the total book volume. The external mass transfer coefficients was 1.4×10^{-3} and 2.7×10^{-2} m/s, for the low and high paper fraction books, respectively. The authors attributed this considerable difference in the parameter to the unevenness of the exposed surface of the low paper fraction book. In turn, Massoquete et al. (2005) used the average k_f value derived from the measurements of water vapour flow in the transverse direction. In this study, we adopted the ‘best-fit’ k_f value of 7×10^{-3} obtained by fitting the curve of the moisture uptake by a book specimen placed in a climatic

chamber with the use of the finite element modelling (see part ‘Moisture uptake by book specimens’ below).

The effective diffusivities in the in-plane direction, calculated with the use of Eq. (7), are listed in Table 3 for different RH gradients and two compression degrees of the specimens. Uncertainty of D_{xy} was 1×10^{-6} m²/s calculated using the propagation of uncertainty method by taking into account the uncertainty of all the variables that were measured in the experiment—time, mass, RH and length.

Several tendencies are evident from the data. Increases of D_{xy} were observed at 75% RH whereas the parameter had constant lower values at dry conditions. The tendency was described earlier by several authors (Gupta and Chatterjee 2003a; Massoquete et al. 2005) and interpreted by a change in the mechanism of water transport through paper. At dry conditions, the water transport is assumed to occur primarily as diffusion of vapour through the pore space, whereas at higher moisture contents, diffusion of water in the condensed phase through the fibre matrix is assumed to become more significant and add to the overall moisture transmission.

Further, it is clear from the data that D_{xy} was affected by the paper fraction in the specimens which were combination of paper sheets and thin air layers or pockets between the sheets. When a specimen is compressed, the thickness of air layers or pockets between the sheets is reduced, paper fraction increases and the diffusivity decreases. Massoquete et al. (2005) determined much lower D_{xy} values of $3\text{--}4 \times 10^{-6}$ m²/s just for the paper structures by introducing the polyisobutylene adhesive between the sheets which blocked any moisture transport through air layers or gaps. Finally, the diffusivities for the more porous, less

Table 3 Effective in-plane diffusivity (D_{xy}) of papers investigated at 22 °C for different RH gradients calculated using Eq. (8) with k_f of 7×10^{-3} m/s

Material type	D_{xy} (10^{-5} m ² /s) (min–max)					
	Desiccant method average RH (%)				Water method average RH (%)	
	25		35		75	
	Loose	Compressed	Loose	Compressed	Loose	Compressed
Paper R4 made of rags, gelatine sized	1.0	0.7	1.0	0.9	1.3	1.3
Paper M4, machine made	0.7	0.6	1.0	0.8	1.0	0.9

dense eighteenth century paper made of rags (R4) are generally higher than for the denser machine-made nineteenth-century material (M4).

Fibre mass transfer coefficient

The rate of water vapour uptake or release by fibres were determined using the linear driving force model:

$$\frac{\partial MC}{\partial t} = k_i(EMC - MC) \tag{9}$$

where MC—moisture content in fibres, EMC—equilibrium moisture content in fibres, k_f —fibre mass transfer coefficient. After integration Eq. (9) becomes:

$$MC = EMC(1 - e^{-k_i t}) \tag{10}$$

k_i determined by least-squares regression of the moisture uptake data on the step change of RH from 0 to 10% to Eq. (10) (Fig. 9) was $3.8 \times 10^{-3} \text{ s}^{-1}$. During the measurement water vapour was introduced under the vacuum condition with no air present in the paper so the adsorption rate reflected only the rate of water vapour uptake by the fibres. The value was very close to $3.5 \times 10^{-3} \text{ s}^{-1}$ determined previously (Bandyopadhyay et al. 2000, 2002).

Moisture uptake by book specimens

Figure 10 shows the plots of transient water uptake by two different book specimens of rather loose arrangement of sheets, exposed to an RH abrupt change from

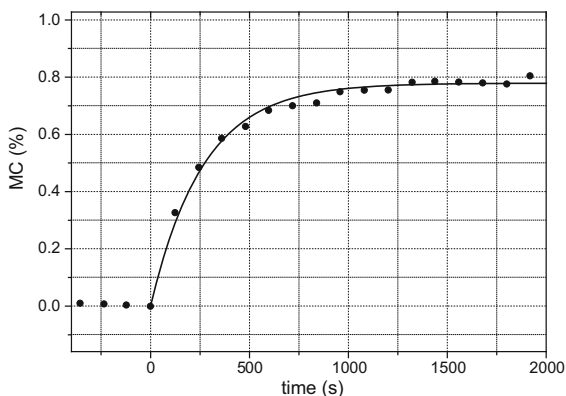


Fig. 9 Experimental data for uptake of water vapour—introduced under vacuum conditions—by paper M4, subjected to a step RH change from dry condition to 10%, are compared with the curve calculated from the least-square regression of the data to Eq. (10)

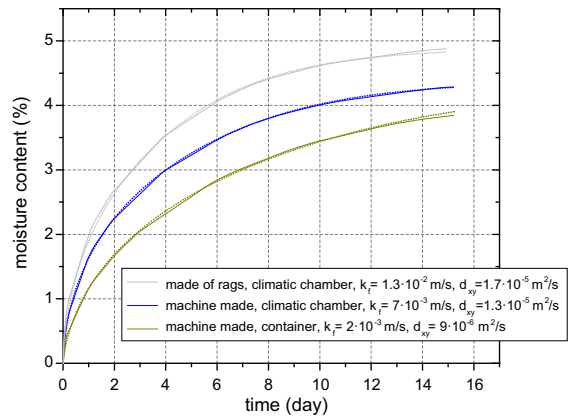


Fig. 10 Gravimetrically measured uptake of water vapour by the book specimens, subjected to a step RH change from dry condition to 43% in a plastic container or a climatic chamber, compared with the numerical simulations

dry condition to 43%, at constant temperature of 22 °C, within a plastic container or a climatic chamber.

The curves were fitted using the finite element modelling of moisture transport to extract the external mass transfer coefficients and the in-plane diffusivities. The following equation governing water vapour transport in the book specimens along paper sheets was used:

$$\rho_p \frac{dEMC(RH)}{dRH} \frac{dRH}{dt} = \nabla \cdot [p_{sat}(T)D_{xy}(RH)\nabla RH] \tag{11}$$

where ρ_p is paper density.

Equation governing water vapour flux at the specimen’s boundary was of the form:

$$-n \cdot (D_{xy}(RH)\nabla RH) = k_f(RH_{ext} - RH) \tag{12}$$

where n is a unit vector normal to the surface and RH_{ext} is external RH.

The approach involved varying k_f and D_{xy} used as the input parameters in the modelling: k_f was varied using logarithmic division and assuming 50 steps per decade in the range of 3×10^{-4} – $1.3 \times 10^{-2} \text{ m/s}$ and D_{xy} was varied using the same method in the range of 3×10^{-6} – $3 \times 10^{-5} \text{ m}^2/\text{s}$. For each pair of k_f and D_{xy} , the R-squared value was calculated. The outcome of the calculation were three pairs of ‘best fit’ external mass transfer coefficients and in-plane diffusivities which minimized the error, indicated in Fig. 10. As expected, the k_f values determined for the

measurements in the climatic chamber—with more intense air movement—shifted to larger values when compared to the measurements in the container. Also, the k_f values for surfaces of paper stacks perpendicular to the paper sheets (Fig. 10) proved to be higher than the k_f range determined for surfaces parallel to the paper sheets (Table 2). Further, the data indicated 9×10^{-6} – 1.7×10^{-5} m²/s as the D_{xy} range, which agrees reasonably with the results of the laboratory measurements of the same parameter shown in Table 3.

Conclusions

There are several significant aspects of this study. Firstly, the analysis of the water sorption isotherms for historical cellulose-based materials—papers and boards—using the Guggenheim-Andersen-de Boer equation has provided a good tool for the comparison of moisture properties of various specimens typical of library or archival collections: gelatin sized materials made of rags and rosin-alum sized wood pulp-based materials obtained in the mechanical or chemical pulping process. It has also been demonstrated that the ‘average’ sorption isotherms can be derived from the sorption data available for various sets of specimens. In particular, the average adsorption curve for all specimens representative of typical library and archive collections was found to be close to that of pure cellulose. Such generalised information can be very useful in modelling buffering capacities of mixed collections stored in libraries and archives. Secondly, in-plane diffusivities along the paper sheets, the primary direction of uptake and release of moisture by books or stack of archival records, were determined. The measurements encompassed not only two principal categories of historical papers—made of rags or based on wood pulp—but also a range of RH levels and paper compression degrees, reflecting for example loose or squeezed books placed next to each other on a bookshelf. It is generally agreed that repositories for archive and library materials should maintain RH optimally below 60% above which level an increasing risk of microbiological activity occurs (ISO11799 2003). At such dry conditions, the in-plane diffusivities fell within a range of 6×10^{-6} – 1.7×10^{-5} m²/s within which higher values characterize loose books and stacks of sheets, and less dense

hand-made papers, whereas lower values characterize squeezed books and denser machine-made papers. Finally, the external mass transfer coefficients at the surface of the paper objects perpendicular to the paper sheets were established to be over 2×10^{-3} m/s, the specific values depending on intensities of air motion which can be expected in typical environments of libraries and archives.

The findings of the study can be put into meaningful synthetic information on the ‘general’ values for the key parameters which can be used in modelling the moisture buffering and response of cellulose-based objects in typical library and archive collections in which books or records are placed next to each other on a bookshelf: *water sorption isotherms characteristic of pure cellulose, in-plane water vapour diffusivity of 1×10^{-5} m²/s and external mass transfer coefficient of 7×10^{-3} m/s*. The data on water sorption can be further used in equations describing the rate of cellulose degradation through the hydrolysis reactions, which critically depends on the water content in paper, next to temperature and concentrations of acids (Strlič 2015).

The present work can be also extended to modelling buffering capacities of paper collections that can be more easily exploited in the practice of humidity control in libraries and archives. As the complex numerical simulations of moisture transport in paper objects require specialized software and high computational load, the moisture uptake and release can be simplified by adopting the effective moisture capacity approach (Janssen and Roels 2009; Steeman et al. 2010). The approach assumes that the moisture mass in the objects is always in equilibrium with the room air. This allows the moisture buffering capacity of the objects and the room air to be integrated by multiplying the moisture capacity of the interior air by a constant multiplication factor. Using the moisture adsorption and diffusion parameters determined in this study attempts will be undertaken to express buffering capacities in the repositories in terms of effective moisture capacity of indoor air for ranges of buildings, collections and time-scales of RH variations.

Acknowledgments The research was supported by Grant PBS2/A9/24/2013 from the Polish National Centre for Research and Development.

Open Access This article is distributed under the terms of the Creative Commons Attribution 4.0 International License (<http://creativecommons.org/licenses/by/4.0/>), which permits unrestricted use, distribution, and reproduction in any medium, provided you give appropriate credit to the original author(s) and the source, provide a link to the Creative Commons license, and indicate if changes were made.

References

- ASTM E96/E96 M-16 (2016) Standard test methods for water vapor transmission in materials
- Bandyopadhyay A, Radhakrishnan H, Ramarao BV, Chatterjee SG (2000) Moisture sorption response of paper subjected to ramp humidity changes. *Ind Eng Chem Res* 39:219–226
- Bandyopadhyay A, Ramarao BV, Ramaswamy S (2002) Transient moisture diffusion through paperboard materials. *Colloids Surf A Physicochem Eng Asp* 206:455–467
- Bedane AH, Xiao H, Eic M, Farmahini-Farahani M (2015) Structural and thermodynamic characterization of modified cellulose fiber-based materials and related interactions with water vapor. *Appl Surf Sci* 351:725–737
- Bedane AH, Eic M, Farmahini-Farahani M, Xiao H (2016) Theoretical modeling of water vapor transport in cellulose-based materials. *Cellulose* 23:1537–1552
- Calvini P, Gorassini A (2002) FTIR – Deconvolution spectra of paper documents. *Restaurator* 23:48–66
- Chatterjee SG (2008) A simple description of transient moisture diffusion in paper. *Indian Chem Eng* 50:34–46
- Derluyn H, Janssen H, Diepens J, Derome D, Carmeliet J (2007) Hygroscopic behavior of paper and books. *J Build Phys* 31:9–34
- Gupta H, Chatterjee SG (2003a) Parallel diffusion of moisture in paper. Part 1: steady-state conditions. *Ind Eng Chem Res* 42:6582–6592
- Gupta H, Chatterjee SG (2003b) Parallel diffusion of moisture in paper. Part 2: transient conditions. *Ind Eng Chem Res* 42:6593–6600
- Hong SH, Strlic M, Ridley I, Ntanos K, Bell N, Cassar M (2012) Climate change mitigation strategies for mechanically controlled repositories: the case of The National Archives, Kew. *Atmos Environ* 49:163–170
- Hubbe M (2011) Internal sizing agents. In: Hagiopol C, Johnston JW (eds) *Chemistry of modern papermaking*. CRC Press Taylor & Francis Group, Boca Raton, pp 267–326
- ISO11799 (2003) Information and documentation – Document storage requirements for archive and library materials
- Janssen H, Roels S (2009) Qualitative and quantitative assessment of interior moisture buffering by enclosures. *Energ Build* 41:382–394
- Jowitt R, Wagstaffe PJ (1989) The certification of the water content of microcrystalline cellulose (MCC) at 10 water activities. BCR information reference materials. Report EUR 12429, Office for Official Publications of the European Communities, Luxembourg
- Kupczak A, Sadłowska-Sałęga A, Krzemień L, Sobczyk J, Radoń J, Kozłowski R (2018) Impact of paper and wooden collections on humidity stability and energy consumption in museum and libraries. *Energ Build* 158:77–85
- Massoquete A, Lavrykov SA, Ramarao BV, Goel A, Ramaswamy S (2005) The effect of pulp refining on lateral and transverse moisture diffusion in paper. *Tappi J* 4:3–8
- Nilsson L, Stenström S (1995) Gas diffusion through sheets of fibrous porous media. *Chem Eng Sci* 50:361–371
- Nilsson L, Wilhelmsson B, Stenström S (1993) The diffusion of water-vapor through pulp and paper. *Dry Tech* 11:1205–1225
- Parker ME, Bronlund JE, Mawson AJ (2006) Moisture sorption isotherms for paper and paperboard in food chain conditions. *Packag Technol Sci* 19:193–209
- Rachwał B, Bratasz Ł, Krzemień L, Łukomski M, Kozłowski R (2012) Fatigue damage of the gesso layer in panel paintings subjected to changing climate conditions. *Strain* 48:474–481
- Ramarao BV, Massoquete A, Lavrykov S, Ramaswamy S (2003) Moisture diffusion inside paper materials in the hygroscopic range and characteristics of diffusivity parameters. *Dry Technol* 21:2007–2056
- Rawat SPS, Khali DP (1999) Studies on adsorption behaviour of water vapour in lignin using the Brunauer-Emmett-Teller theory. *Holz Roh Werkst* 57:203–204
- Rouchon V, Pellizzi E, Janssens K (2010) FTIR techniques applied to the detection of gelatin in paper artifacts: from macroscopic to microscopic approach. *Appl Phys A* 100:663–669
- Sedlbauer K (2002) Prediction of mould growth by hygrothermal calculation. *J Build Phys* 25:321–326
- Sing KSW, Everett DH, Haul RAW, Moscou L, Pierotti RA, Rouquerol J, Siemieniewska T (1985) Reporting physisorption data for gas solid systems with special reference to the determination of surface-area and porosity. *Pure Appl Chem* 57:603–619
- Staniforth S (2014) Environmental conditions for the safeguarding of collections: future trends. *Stud Conserv* 59:213–217
- Steeman M, De Paepe M, Janssens A (2010) Impact of whole-building hygrothermal modelling on the assessment of indoor climate in a library building. *Build Environ* 45:1641–1652
- Strlič M (2015) Damage function for historic paper. Part III: Isochrones and demography of collections. *Herit Sci* 3:40
- Timmermann EO (2003) Multilayer sorption parameters: BET or GAB values? *Coll Surf A* 220:235–260
- Volkova N, Ibrahim V, Hatti-Kaul R, Wadsö L (2012) Water sorption isotherms of Kraft lignin and its composites. *Carbohydr Polym* 87:1817–1821